

Accepted Article

Title: Isolated Zn-Co Atomic Pair for Highly Active and Durable Oxygen Reduction

Authors: Ziyang Lu, Bo Wang, Yongfeng Hu, Wei Liu, Yufeng Zhao, Ruouo Yang, Zhiping Li, Jun Luo, Bin Chi, Zheng Jiang, Minsi Li, Shichun Mu, Shijun Liao, Jiujun Zhang, and Xueliang Sun

This manuscript has been accepted after peer review and appears as an Accepted Article online prior to editing, proofing, and formal publication of the final Version of Record (VoR). This work is currently citable by using the Digital Object Identifier (DOI) given below. The VoR will be published online in Early View as soon as possible and may be different to this Accepted Article as a result of editing. Readers should obtain the VoR from the journal website shown below when it is published to ensure accuracy of information. The authors are responsible for the content of this Accepted Article.

To be cited as: *Angew. Chem. Int. Ed.* 10.1002/anie.201810175
Angew. Chem. 10.1002/ange.201810175

Link to VoR: <http://dx.doi.org/10.1002/anie.201810175>
<http://dx.doi.org/10.1002/ange.201810175>

Isolated Zn-Co Atomic Pair for Highly Active and Durable Oxygen Reduction

Ziyang Lu⁺, Bo Wang⁺, Yongfeng Hu⁺, Wei Liu⁺, Yufeng Zhao^{*}, Ruouo Yang, Zhiping Li, Jun Luo^{*}, Bin Chi, Zheng Jiang^{*}, Minsi Li, Shichun Mu, Shijun Liao, Jiuju Zhang, Xueliang Sun^{*}

Abstract: N-coordinated nonprecious dual metal catalysts have demonstrated superior catalytic activity by offering more concentrated active sites. However a rational design of such system remains conceptually challenging which requires in-depth research both experimentally and theoretically. Herein, we develop a competitive complexation strategy to construct a novel electrocatalyst with Zn-Co atomic pairs coordinated on N doped carbon support (Zn/CoN-C). Such architecture offers enhanced binding ability of O₂, significantly elongates the O-O length (from 1.23 Å to 1.42 Å), and thus facilitates the cleavage of O-O bond, showing a theoretical overpotential of 0.335V during ORR process. As a result, the Zn/CoN-C catalyst exhibits outstanding ORR performance in both alkaline and acid conditions with a half-wave potential of 0.861 and 0.796 V respectively. The assembled zinc-air battery with Zn/CoN-C as cathode catalyst presents a maximum power density of 230 mW cm⁻² along with excellent operation durability. The excellent catalytic activity in acid is also verified by H₂/O₂ fuel cell tests (peak power density of 705 mW cm⁻²).

Electrochemical oxygen reduction reaction (ORR) has gained widespread attentions due to its significance in electrochemical energy storage and conversion including proton-conducting

membrane fuel cells or metal-air batteries.^[1] Platinum-based catalysts are generally efficient for ORR, but their wider applicabilities are restricted by its high price, and limited stability.^[2] Replacement of noble metal materials with less expensive, highly active and durable electrocatalysts for ORR is thereby increasingly attractive but arduous with great challenges ahead.

Nonprecious metal catalysts with M-N_x-C (M stands for nonprecious metal elements) coordination, represent a new type of effective catalysts as possible alternatives to Pt.^[3] Recent study found that, achieving atomic-level regulation of metal atoms is critical to designing high catalytic active catalysts.^[4] Isolated single-atom iron or cobalt catalysts supported on carbon materials have demonstrated unexpected ORR reactivity than commercial Pt/C.^[5] Follow-up study revealed that, catalysts with bimetallic or multimetallic active sites can further enhance the catalytic activity and selectivity in numerous catalytic conversion reactions.^[6] A recently reported Pt free catalyst with N-coordinated Fe-Co dual sites delivers outstanding activity for ORR in acidic electrolyte.^[7] Compared to the single metallic site, the structure formed by the coordination of dual-metal-atom with nitrogen atoms is more favorable for cracking O₂ bond.^[8] Nevertheless, the current research efforts about M-N_x-C catalysts mainly focused on Ni, Co or Fe/N-doped carbon materials catalysts.^[9,10] Exploring new metal components and new catalytic site may be an effective way to increase catalytic activity under the premise of ensuring high dispersion. In nature, besides Fe and Co porphyrin, Zn porphyrin structure can also be found in carbonic anhydrase with four-coordinated structure.^[11] In view of that, Zn has a smaller electronegativity ($\chi=1.65$) compared to Fe ($\chi=1.83$) and Co ($\chi=1.88$) which makes it easier to donate its outer electron. When atomic pairs formed between Zn and Co or Fe, the interactions between the electronic structures might result in a more optimized structure, which makes it possible for the adsorption and desorption of the reaction intermediate to reach a suitable state, so that the diatomic pair has a higher catalytic activity. Thereby, introducing more metal species to construct bimetallic or multimetallic active sites are challenging yet of great significance to achieve best performing catalysts.

Herein, we report a new design of discrete Zn, Co bimetallic sites supported on N doped carbon through a competitive complexation strategy, whereby chitosan was used as C and N sources, zinc chloride, and cobalt acetate are selected as metal precursors (**Figure 1a**). The 4s and 4p electrons of Co²⁺ or Zn²⁺ can be coordinated with the -NH₂ and -OH group on chitosan chains through a simultaneous competitive complexation process, thus allowing the homogeneous dispersion of Zn/Co. And due to their similar coordination abilities,^[12] a bimetallic

- [*] Z. Lu, B. Wang, Z. Li, Prof. Y. Zhao
Key Laboratory of Applied Chemistry in Hebei Province, Yanshan University
Qinhuangdao 066004, China
E-mail: yufengzhao@ysu.edu.cn
Prof. Y. Zhao, Prof. J. Zhang
Institute of Sustainable Energy, Shanghai University, Shanghai, 200444, P. R. China.
Prof. X. Sun, M. Li
Department of Mechanical and Materials Engineering, University of Western Ontario, London, Ontario N6A 5B9, Canada.
E-mail: xsun@eng.uwo.ca
Y. Hu
Canadian Light Source, 44 Innovation Boulevard, Saskatoon, SK S7N 2 V3, Canada
Prof. J. Luo, W. Liu
Tianjin Key Lab of Advanced Functional Porous Materials, Tianjin University of Technology, Tianjin 300384, China.
E-mail: jluo@tjut.edu.cn
Prof. Z., Jiang, R. Yang
Shanghai Synchrotron Radiation Facility, Chinese Academy of Sciences, shanghai 201204, China
Email jiangzheng@sinap.ac.cn
Prof. S. Mu
Key Laboratory of Advanced Technology for Materials Synthesis and Processing, Wuhan University of Technology, Wuhan 430070, China
Prof. S. Liao, B. Chi
The Key Laboratory of Fuel Cell Technology of Guangdong Province South China University of Technology, Guangzhou 510641, China.
- [*] These authors contribute equally to this work.
Supporting information for this article is given via a link at the end of the document.

Zn/CoN_x-C nanostructure with atomic dispersion is finally achieved after pyrolysis at 750°C, which is denoted as Zn/CoN-C. The weight percentage of Zn, Co is determined as 0.33 wt% and 0.14 wt% respectively, by inductively coupled plasma mass spectrometry (ICP-MS). This synthetic method allows scalable synthesis of catalysts with good reproducibility.

In order to confirm the existential form of Zn and Co dual atoms, we carried out aberration-corrected atomic-resolution high-angle annular dark field scanning transmission electron microscopy (HAADF-STEM) measurements (Figure 1b). Small bright spots are evenly distributed in carbon substrate, which are attributed to the relatively high atomic numbers of Zn and Co. Further enhancing the magnification, small bright dual dots can be observed more clearly (Figure 1c), in which Zn/Co atomic pair can be recognized by bright spots marked with red circles. Some individual Zn or Co atoms can be distinguished and marked with

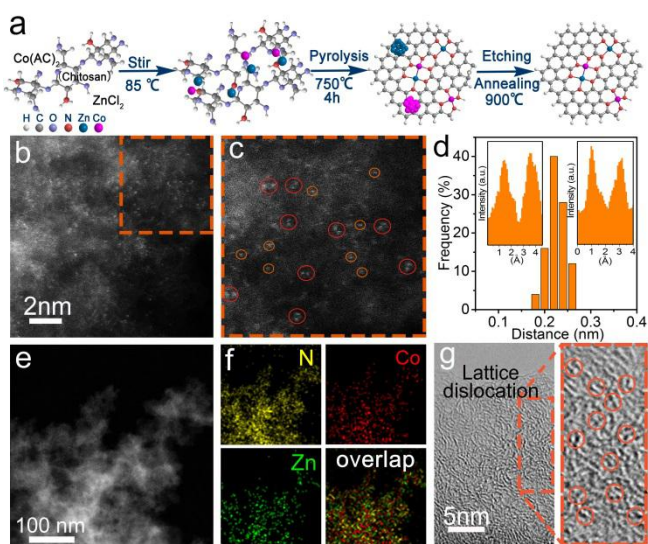


Figure 1. (a) Schematic illustration of the formation of Zn/CoN-C. Aberration-corrected HAADF-STEM image (b) and enlarged images (c) of the Zn/CoN-C. In (c), some of bimetallic Zn/Co sites are highlighted by larger red circles, and some of single Co/Zn atoms highlighted by smaller orange circles. (d) Statistical Zn-Co distance in the observed diatomic pairs, in which the two insets are intensity profiles obtained on two bimetallic Co/Zn sites. HAADF-STEM image (e) and corresponding element maps (f), showing the distribution of N, Zn, and Co. (g) HR-TEM of Zn/CoN-C, in which some lattice distortions are highlighted by orange circles.

orange circles. Statistical analysis of more than 40 pairs of dual atoms showed a Zn-Co distance of 0.22 ± 0.04 nm (Figure 1d). The well dispersed Zn-Co dual-sites can be clearly identified in accessional intensity profiles (Figure 1d insets). HAADF-STEM (Figure 1e) and elemental mapping (Figure 1f and S1) reveal that N, Zn and Co are homogeneously distributed in the Zn/CoN-C. The (HR) TEM image (Figure 1g) demonstrates lattice distortion defects characteristic, which might be attributed to the coordination of single or dual zinc/cobalt atoms with nitrogen. For comparison, single-metal atom Co or Zn doped catalysts, denoted as CoN-C and ZnN-C were also synthesized through similar approaches.

X-ray diffraction (XRD) patterns of the samples (Figure S2) confirm the non-formation of metallic and oxide crystals on carbon supports. Nitrogen adsorption measurement illustrates the high BET (Brunauer-Emmet-Teller) specific surface area ($1343 \text{ m}^2/\text{g}$) of Zn/CoN-C with an average pore width of 2.46 nm (Figure S3). Raman spectra (Figure S4) and XPS spectrum of C1s (Figure S5) suggest that more defects are produced due to the co-coordination between Co and Zn and the N doped carbon support, which plays an important role in the electronic properties of carbon matrix. As shown in Figure S6, N1s spectrum for Zn/CoN-C can be deconvoluted into four peaks, pyridinic N (398.3 eV), N-Zn/Co (399.7 eV), pyrrolic N (400.6 eV), and graphitic N (401.4 eV), respectively. The existence of N-Zn/Co can also be confirmed at Zn 2p spectrum (Figure S7b) and Co 2p_{1/2} signals at 778.7 eV. (Figure S7c).^[5b]

X-ray absorption near-edge structure (XANES) and extended X-ray absorption fine structure measurements (EXAFS) were conducted to investigate the chemical state and coordination environment of Co and Zn atoms in the catalysts. As shown in the XANES spectra (Figure 2a), the absorption edge of Co K-edge of CoN-C shifted 3.0 eV towards lower energy relative to CoO, indicating that the valence state of CoN-C is situated between that of Co⁰ and Co^{II}. Furthermore, from the EXAFS spectra of different samples (Figure 2b), a main peak at about 1.5 Å can be observed for both cobalt phthalocyanine (CoPc) and CoN-C, which is typically assigned to the Co-N coordination, demonstrating the confined Co-N4 coordination environment in CoN-C. The Co K-edge EXAFS spectrum of Zn/CoN-C is characterized by three peaks at 1.4 Å, 2.1 Å and 2.4 Å, corresponding to the nearest Co-N, next nearest Co-Metal and long range Co-C coordination, respectively (Figure 2b). From its corresponding Zn K-edge XANES spectrum (Figure 2c), we can see that both the edge position and the peak intensity of Zn/CoN-C located between Zn foil and ZnO, which suggests the electronic state of the Zn species is between Zn⁰ and Zn^{II}. On the other hand, Zn K-edge EXAFS (Figure 2d) analysis clearly indicates that Zn/CoN-C and zinc phthalocyanine show a similar main peak at 1.44 Å, which could be attributed to Zn-N scattering paths. The two peaks at 2.1 Å and 2.4 Å, should be due to the next nearest Zn-Metal and long range Zn-C coordinations, respectively.

The fitting results of Zn/CoN-C can better reveal the structural information of the material (Figure S8). The Co-N coordination number is 3.5 for Zn/CoN-C suggest that the catalyst was dominated by the Co-N interaction with a mixed Co-N3 and Co-N4 environment. The second shell coordination number of Co-M is given by $\text{CN}_{\text{Co-M}} = 0.5 \pm 0.1$, suggesting a weak Co-M interaction in form of ZnCoN6 structure. Similarly for Zn of the Zn/CoN-C, it is dominated by the Zn-N coordination (N=3.5) in the first shell, together with a weak second shell due to the Zn-M ($\text{CN}_{\text{Zn-M}} = 0.5 \pm 0.1$), further demonstrating the existence of ZnCoN6 structure in Zn/CoN-C. This result is also consistent with the DFT calculations that Zn and Co are bonded, the system has the lowest energy, therefore Zn and Co tend to form Co-Zn diatomic pairs (Figure S9).

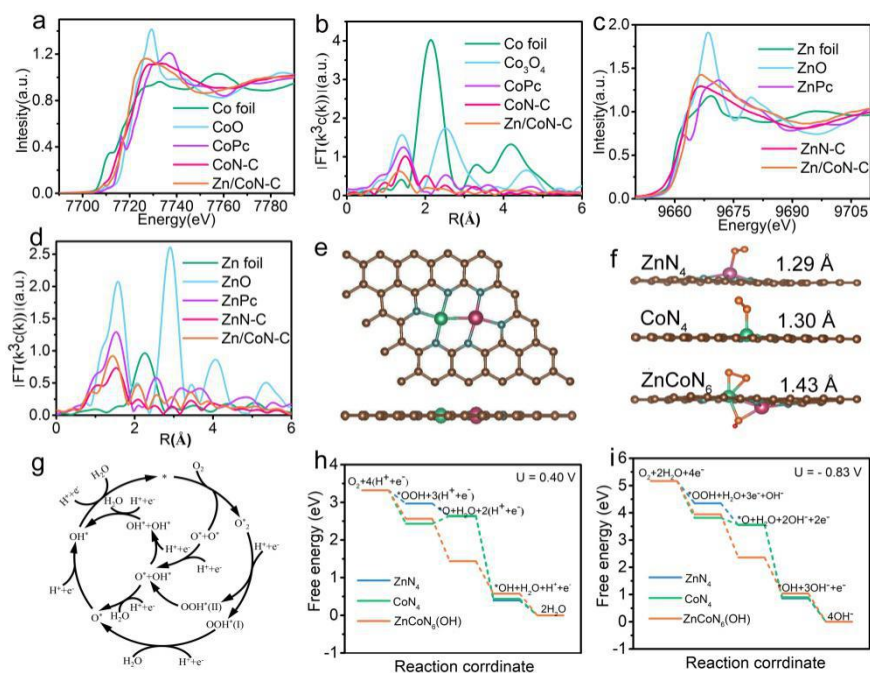


Figure 2. (a) Co K-edge XANES and (b) Fourier-transform EXAFS spectra of Zn/CoN-C and reference samples. (c) Zn K-edge XANES and (d) Fourier-transform EXAFS spectra of Zn/CoN-C and reference samples. (e) Relative position of Zn, Co and N for the Zn/CoN-C considered in the calculations. (f) Optimized geometry of O₂ adsorption configuration on the ZnN₄, CoN₄ and ZnCoN₆(OH) systems. Brown, blue, yellow, green, purple and red balls are C, N, O, Zn, Co and H atoms, respectively. (g) Schematic free energy profiles for the ORR pathway in acidic conditions. (h, i) Free energy diagram for the ZnN₄, CoN₄ and ZnCoN₆(OH) systems during the ORR under acidic and alkaline conditions at U = 0.40 and U = -0.83 V respectively.

DFT calculations were conducted to understand the ORR reactive nature of Zn/CoN-C. It reveals that, due to the co-coordination of bimetallic Zn and Co with N, the electronic structure of the catalyst is modulated, whereby the O-O bond is significantly elongated from 1.23 Å to 1.43 Å after the adsorption of O₂ on ZnCoN₆(OH) sites (Figure 2f). This would facilitate the cracking of O₂ and lead to the reduced dissociation energy barrier,^[7,13] thus efficiently enhancing the ORR activity. As contrast, the O-O bond is only 1.29 Å and 1.30 Å (Figure 2f), after O₂ adsorbed on ZnN₄ and CoN₄ in gas-phase, respectively. Furthermore, it is found that the *OH reduction on ZnCoN₆ is an exothermic process with high stability, which enables the *OH to act as a modifying ligand forming a ZnCoN₆(OH) structure, which remains stable during the entire ORR process.^[8] Unlike under alkaline condition, there are more complex reaction paths under acidic conditions (Figure 2g). Five possible reaction pathways were evaluated in acidic condition. And the reaction mechanism under acidic conditions is also considered (Figure 2h), the ORR process at U = 0.4V in different structures with O₂ → *O₂ → *OOH → *O → *OH → H₂O, reaction path. All reactions are exothermic in view of the fact that all the elementary reaction steps are downhill for ZnCoN₆(OH). Furthermore, ZnCoN₆(OH) shows similar behavior under alkaline condition (Figure 2i). At U = -0.83 V, for Zn/CoN-C, the free energy of all reaction steps also shows strong exothermicities for all elementary reaction steps. The overpotential (η)^[14] of ZnCoN₆(OH) under alkaline condition was 0.335V, which is superior to that of ZnN₄ (0.436V), CoN₄ (0.391V) and

commercial Pt/C (0.45V), suggesting the high ORR catalytic activity of Zn/CoN-C.

The ORR catalytic activity of Zn/CoN-C was investigated in O₂-saturated 0.1M KOH with rotating disk electrode (RDE). At 750 °C the Zn/CoN-C exhibit the optimal electrocatalytic performance as shown in Figure S10. And Cyclic voltammetry (CV) reveals a significant reduction peak at 0.84V for Zn/CoN-C (Figure S11), suggesting a good ORR electrocatalytic activity. The linear sweep voltammetry (LSV) measurements (Figure 3a) show that Zn/CoN-C presents the best oxygen reduction activity, with a much more positive E_{onset} (1.004 V) than Pt/C (0.970 V) and a high E_{1/2} of 0.861V, which is 35 mV more positive than Pt/C. This E_{1/2} value also surpasses those of CoN-C (0.793V) and ZnN-C (0.706V) (Figure 3b). In addition, Zn/CoN-C exhibits a more active J_L of 6.1 mA/cm², and this value is far better than those of Pt/C (5.3 mA/cm²), CoN-C (4.7 mA/cm²) and ZnN-C (4.4 mA/cm²). The catalytic activities of Zn/CoN-C with the optimal Zn-Co atomic ratio (Figure S12) surpass those of most non-precious metal ORR electrocatalysts (Table S1). The electron transfer number of Zn/CoN-C was also evaluated from the LSVs (Figure 3c) according to Koutecky-Levich (K-L) equation, giving the n value of 3.88. The n and H₂O₂ yield were further evaluated through rotating ring-disk electrode (RRDE, Figure 3d), whereby the direct four electron process is confirmed, with n approaching 4 and H₂O₂ yield of about 5%. Tafel plots demonstrate much smaller slope of 67 mV dec⁻¹ of Zn/CoN-C, indicating the superior reaction kinetics (Figure 3e). The durability of Zn/CoN-C was evaluated by CV at a sweep rate of 100 mV/s. After 5000 continuous cycles (Figure 3f), there was 5 mV change in E_{1/2}, and after 10000 cycles, there was only 9 mV change in E_{1/2}, demonstrating that the Zn/CoN-C had the superb stability. And the Zn-Co atomic pairs of the Zn/CoN-C are still well preserved after 10000 cycles of testing, which is verified by HAADF-STEM (Figure S13) and XANES (Figure S14). Furthermore, the in situ XANES spectra of Zn/CoN-C (Figure S15) suggests that Co is more actively involved, and function as active center during the ORR, which likely undergoes a slight redox switch, in agreement with the FeN₄ system.^[15] Upon the closer inspection of the Co K-edge result, the Co K-edge is slowly shifting to higher energy as the potential increases. After the oxygen reduction process, the structure of the Zn/CoN-C has not changed substantially whether for Co K-edge or Zn K-edge, during the whole ORR process which guarantees the high oxygen reduction activity. The fuel crossover effect evaluation of Zn/CoN-C demonstrates excellent tolerance to methanol (Figure S16) and SCN⁻ ions (Figure S17).^[5a, 16-17]

A primary Zn-air battery was assembled to evaluate the practical application of Zn/CoN-C. Significantly, a maximum power of 230 mW cm⁻² is achieved from the battery using Zn/CoN-C catalyst

(Figure 4a) outperforming the Pt/C based counterpart (201 mW cm⁻²) and most of previous works (Table S2, Figure S18).

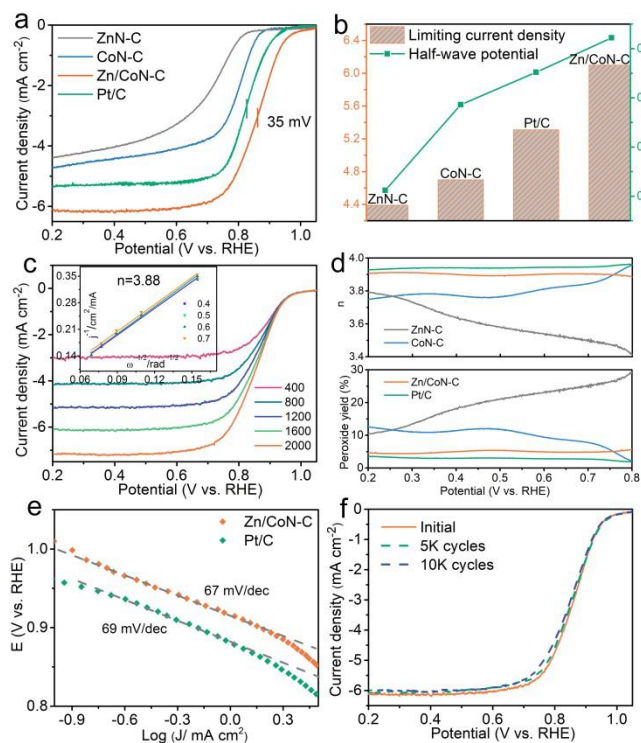


Figure 3. (a) ORR Linear scan voltammogram (LSV) curves for different catalysts in O₂ saturated 0.1 M KOH solution. (b) Limit current density and half-wave potential for different catalysts. (c) LSV curves for Zn/CoN-C at different rotating rates from 400 to 2000 rpm and the inset is K-L plots at various potentials. (d) Electron transfer number and H₂O₂ yield for different catalysts. (e) Corresponding Tafel plots obtained from the RDE polarization curves. (f) The durability tests of Zn/CoN-C.

Furthermore, no significant potential change was detected at a current density of 5 mA cm⁻² for 100000s (Figure 4b), indicating a stable practical application performance. As shown in Figure 4b inset, two series-connected Zn-air batteries based on the Zn/CoN-C as cathode can power a series of red light-emitting diode (LED) in parallel (LED, 2.2 V) with an outstanding stability.

Promisingly, the Zn/CoN-C also presents outstanding ORR activity in acidic conditions. In 0.1M HClO₄, Zn/CoN-C shows a considerably high ORR catalytic activity with E_{1/2} of 0.796 V and E_{onset} of 0.97 V, which is comparable to that of Pt/C (Figure 4c), and superior to most of non-precious metal ORR electrocatalysts (Table S3). And after 10000 cycles of CV, there was no obvious change in E_{1/2}, demonstrating the excellent stability of Zn/CoN-C (Figure S19). In the SCN⁻ poisoning test (Figure S20), the E_{1/2} of Zn/CoN-C negatively shifted by 30 mV and the E_{onset} remained unchanged after adding SCN⁻. This apparent resistance to SCN⁻ poisoning can be attributed to the bimetallic coordination in the ZnCoN₆ structure that regulates the interfacial electron structure, which is detrimental to the binding to KSCN. These test results clearly show that dual-metal sites ZnCoN₆ are the major active sites. A H₂/O₂ fuel cell was

assembled to verify the practical application potential in acidic solution. As a result, a kinetic current of 999 mA cm⁻² is achieved at 0.6 V and a peak power density of 705 mW cm⁻² at 0.5 V, which is ~78% of that based on commercial Pt/C (Figure 4d). Furthermore, after eight hours of stability testing, there was no attenuation of activity (Figure S21).

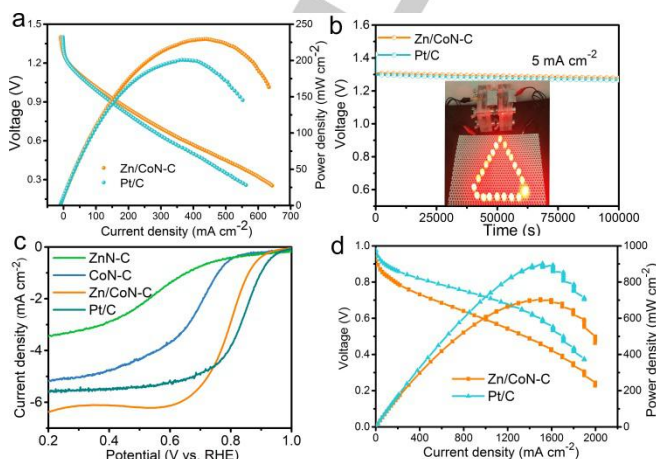


Figure 4. (a) Polarization and power density curves of primary Zn-air batteries using Zn/CoN-C and Pt/C as ORR catalyst in 6 M KOH electrolyte. (b) Galvanostatic discharge of the fabricated Zn-air batteries and the inset is the photograph of a series of LED powered by two liquid Zn-air batteries in series. (c) ORR Linear scan voltammogram (LSV) curves for different catalysts in 0.1 M HClO₄ solution. (d) H₂/O₂ fuel cell polarization plots.

In summary, this work demonstrates that the Zn/Co dual atoms sites can serve as efficient ORR catalyst with outstanding activity both experimentally and theoretically. The Zn/Co dual atoms sites were confirmed by a combination of aberration-corrected HAADF-STEM, XAFS and DFT calculations. DFT calculations show that ZnCoN₆ site is the main active site and the theoretical overpotential of oxygen reduction can be as low as 0.335V. In addition, the catalytic activity can be maintained even under acidic environment. Furthermore, the assembled Zn-air batteries and fuel cell with Zn/CoN-C as catalyst show excellent power density and stability, which demonstrates the practical application of the as-prepared Zn/CoN-C catalysts for both fundamental research and practical applications.

Acknowledgements

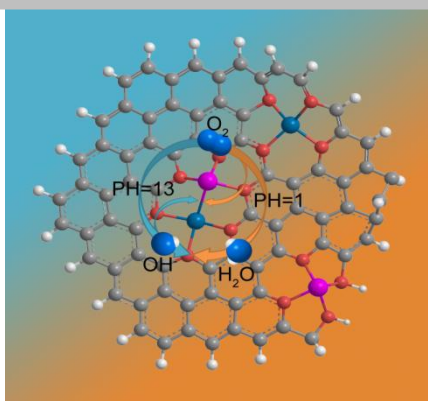
We thank the financial supports from NSFC (51774251), HB NSFDYS (B2017203313), HEITSP (SLRC2017057), and National Program for Thousand Young Talents of China. The XAS measurement was conducted at the Canadian Light Source (CLS). CLS is supported by the NSERC, NRC, CIHR of Canada, the University of Saskatchewan, and the BL 14W beamline at the Shanghai Synchrotron Radiation Facility (SSRF).

Keywords: isolated atomic pair, M-N_x-C, oxygen reduction reaction, Zn-air battery

- [1] a) J. A. Asensio, E. M. Sánchez, P. Gómezromero, *Chem. Soc. Rev.* **2010**, *41*, 3210-3239; b) J. Miyake, R. Taki, T. Mochizuki, R. Shimizu, R. Akiyama, M. Uchida, K. Miyatake, *Science Advances* **2017**, *3*, eaao0476; c) Z. Zhao, M. Li, L. Zhang, L. Dai, Z. Xia, *Adv.Mater.* **2016**, *27*, 6834-6840; d) W. D. N. Jia, M. Tang, T. F. Jaramillo, *Energy Environ. Sci.* **2014**, *7*, 2017-2024.
- [2] a) B. Y. Xia, Y. Yan, N. Li, H. B. Wu, X. W. Lou, X. Wang, *Nat. Energy* **2016**, *1*, 15006; b) T. Y. Ma, J. Ran, S. Dai, M. Jaroniec, S. Z. Qiao, *Angew.Chem. Int. Ed.* **2015**, *54*, 4646-4650; c) K. Gong, F. Du, Z. Xia, M. Durstock, L. Dai, *Science* **2009**, *323*, 760-764; d) Y. Liang, Y. Li, H. Wang, J. Zhou, J. Wang, T. Regier, H. Dai, *Nat. Mater.* **2011**, *10*, 780.
- [3] a) S. Yasuda, A. Furuya, Y. Uchibori, J. Kim, K. Murakoshi, *Adv. Funct. Mater.* **2016**, *26*, 738-744; b) A. Zitolo, N. Ranjbarsahraie, T. Mineva, J. Li, Q. Jia, S. Stamatini, G. F. Harrington, S. M. Lyth, P. Krtil, S. Mukerjee, *Nat. Commun.* **2017**, *8*, 957; c) J. Wei, Y. Liang, Y. Hu, B. Kong, G. P. Simon, J. Zhang, S. P. Jiang, H. Wang, *Angew.Chem. Int. Ed.* **2016**, *128*, 1377-1381; d) Z. Huang, H. Pan, W. Yang, H. Zhou, N. Gao, C. Fu, S. Li, H. Li, Y. Kuang, *ACS nano* **2018**; e) A. Zitolo, V. Goellner, V. Armel, M. T. Sougrati, T. Mineva, L. Stievano, E. Fonda, F. Jaouen, *Nat. Mater.* **2015**, *14*, 937.
- [4] a) C. Zhu, S. Fu, Q. Shi, D. Du, Y. Lin, *Angew.Chem. Int. Ed.* **2017**, *56*, 13944-13960; b) Q. Cheng, L. Yang, L. Zou, Z. Zou, C. Chen, Z. Hu, H. Yang, *Acs Catal* **2017** *7*, 6864-6871.
- [5] a) Y. Chen, S. Ji, Y. Wang, J. Dong, W. Chen, Z. Li, R. Shen, L. Zheng, Z. Zhuang, D. D. Wang, Y. D. Li, *Angew.Chem.* **2017**, *129*, 7041-7045; b) P. Yin, T. Yao, Y. Wu, L. Zheng, Y. Lin, W. Liu, H. Ju, J. Zhu, X. Hong, Z. Deng, *Angew.Chem.* **2016**, *128*, 10958-10963.
- [6] a) H. Tang, S. Cai, S. Xie, Z. Wang, Y. Tong, P. Mu, X. Lu, *Advanced Science* **2016**, *3*, 1487-1498; b) B. Y. Guan, Y. Lu, Y. Wang, M. Wu, X. W. Lou, *Adv. Funct. Mater.* **2018**, *28*, 1706738; c) J. Jung, K. Song, Y. Bae, S. I. Choi, M. Park, E. Cho, K. Kang, Y. M. Kang, *Nano Energy* **2015**, *18*, 71-80; d) M. Kodali, C. Santoro, S. Herrera, A. Serov, P. Atanassov, *J. Power Sources* **2017**, *366*, 18-26.
- [7] J. Wang, Z. Huang, W. Liu, C. R. Chang, H. Tang, Z. Li, W. Chen, C. Jia, T. Yao, S. Wei, *J. Am. Chem.Soc.* **2017**, *139*, 17281-17284.
- [8] a) M. Xiao, H. Zhang, Y. Chen, J. Zhu, L. Gao, Z. Jin, J. Ge, Z. Jiang, S. Chen, C. Liu, *Nano Energy* **2018**, *46*, 396-403; b) E. F. Holby, C. D. Taylor, *Sci Rep* **2015**, *5*, 9286.
- [9] a) G. Zhang, W. Lu, F. Cao, Z. Xiao, X. Zheng, *J. Power Sources* **2016**, *302*, 114-125; b) M. Zeng, Y. Liu, F. Zhao, K. Nie, N. Han, X. Wang, W. Huang, X. Song, J. Zhong, Y. Li, *Adv. Funct. Mater.* **2016**, *26*, 4397-4404; c) D. Deng, L. Yu, X. Chen, G. Wang, L. Jin, X. Pan, J. Deng, G. Sun, X. Bao, *Angew. Chem.* **2013**, *125*, 389-393; d) Z. Y. Wu, X. X. Xu, B. C. Hu, H. W. Liang, Y. Lin, L. F. Chen, S. H. Yu, *Angew.Chem.* **2015**, *127*, 8297-8301.
- [10] a) Q. Lai, L. Zheng, Y. Liang, J. He, J. Zhao, J. Chen, *Acs Catal* **2017** *7*, 1655-1663; b) Y. J. Sa, D. J. Seo, J. Woo, J. T. Lim, J. Y. Cheon, S. Y. Yang, J. M. Lee, D. Kang, T. J. Shin, H. S. Shin, *J. Am. Chem.Soc.* **2016**, *138*, 15046-15056; c) J. H. Lee, M. J. Park, S. J. Yoo, J. H. Jang, H. J. Kim, S. W. Nam, C. W. Yoon, J. Y. Kim, *Nanoscale* **2015**, *7*, 10334-10339; d) B. Y. Guan, L. Yu, X. W. Lou, *Advanced Science* **2017**, *4*, 1700247.
- [11] P. Song, M. Luo, X. Liu, W. Xing, W. Xu, Z. Jiang, L. Gu, *Adv. Funct. Mater.* **2017**, *27*, 1700802.
- [12] a) H.-M. Guan, X.-S. Cheng, *Polym. Adv. Technol.* **2004**, *15*: 89-92; b) X. Wang, Y. Du, H. Liu, *Carbohydr. Polym.* **2004**, *56*, 21-26.
- [13] D. H. Lim, J. Wilcox, *J.Phys.Chem. C* **2011**, *115*, 22742-22747.
- [14] a) J. Zhang, Z. Zhao, Z. Xia, L. Dai, *Nat. Nanotech.* **2015**, *10*, 444-452; b) Z. Liu, F. Sun, L. Gu, G. Chen, T. Shang, J. Liu, Z. Le, X. Li, H. B. Wu, Y. Lu, *Adv.Energy Mater.* **2017**, *7*, 1701154.
- [15] Q. Jia, N. Ramaswamy, H. Hafiz, U. Tylus, K. Strickland, G. Wu, B. Barbiellini, A. Bansil, E. F. Holby, P. Zelenay, *Acs Nano* **2015**, *9*, 12496-12505.
- [16] M. S. Thorum, J. M. Hankett, A. A. Gewirth, *J.Phys.Chem.Lett* **2015**, *2*, 295-298.
- [17] C. Zhang, Y. C. Wang, B. An, R. Huang, C. Wang, Z. Zhou, W. Lin, *Adv.Mater.* **2017**, *29*, 1604556

COMMUNICATION

The discrete zinc, cobalt bimetallic sites supported on N doped carbon (Zn/CoN-C) through a competitive complexation strategy. The as-prepared Zn/CoN-C catalyst exhibits outstanding ORR performance in both alkaline and acid conditions, and the assembled Zn-air batteries and H₂/O₂ fuel cell show excellent power density and stability which demonstrate the practical applications.



Ziyang Lu[‡], Bo Wang[‡], Yongfeng Hu[‡], Wei Liu[‡], Yufeng Zhao*, Ruouo Yang, Zhiping Li, Jun Luo*, Bin Chi, Zheng Jiang*, Minsi Li, Shichun Mu, Shijun Liao, Jiujuan Zhang, Xueliang Sun*

Page No. – Page No.

Title

Accepted Manuscript